Adhesion Energy Hysteresis and Friction between Ultrathin Polyglutamate Films Measured with the Surface Forces Apparatus

F.-J. Schmitt,*,† H. Yoshizawa,† A. Schmidt,‡ G. Duda,‡ W. Knoll,‡ G. Wegner,‡ and J. Israelachvili†

Department of Chemical Engineering, and Materials Department, University of California, Santa Barbara, California 93106-5080, and Max-Planck-Institut für Polymerforschung, Ackermannweg 10, D-55021 Mainz, Germany

Received August 12, 1994; Revised Manuscript Received January 3, 1995[⊗]

ABSTRACT: Adhesion and friction forces between deposited monolayers of poly(γ-methyl L-glutamate)$_x$-*co*-(γ-*n*-octadecyl L-glutamate)$_y$—a "hairy rod" polymer having a rigid main chain rod and alkyl side chains containing either 1 or 18 C atoms—were measured using the surface forces apparatus technique. By performing dynamic (time-dependent) adhesion energy and friction experiments as a function of temperature T, we obtained the energy loss spectra for these quasi two-dimensional films. The measured adhesion energy losses or hysteresis as a function of temperature are shown to be related to the interdigitation of the octadecyl side chains, caused by different molecular motions that have been previously shown to be active at different temperatures. Friction experiments probed the energy dissipation processes arising from lateral motion. Assuming that the molecular dissipation processes are the same in both types of measurements (adhesion and friction), we used a previously derived simple formula to relate quantitatively the adhesion energy hysteresis and friction forces.

Introduction

The Langmuir−Blodgett (LB) and self-assembly techniques have gained much interest in the past decades because they offer a unique approach for the construction of 3D superstructures of molecularly thin films.[1] These films are usually formed by amphiphilic molecules, which are ordered in quasi two-dimensional arrays. With the ability to build in functional groups, the construction of sophisticated molecular devices now seems to be feasible, with potential applications in optics, electronics, and tribology and as sensor devices.[2] Unfortunately, in many cases, performance has not been as good as anticipated, LB films especially often lack long time stability, and many of their properties are determined by defects. Thus, it can be concluded that to control or to optimize the properties of LB films, one has first to be able to better control their structure at the molecular level. Even more important is the understanding of how the structure and function of ultrathin films are related, that is, how the molecular-scale properties determine the macroscopic, measurable properties.

One approach for overcoming the limitations of conventional LB films has been the introduction of "hairy rod" type polymers.[3] These macromolecules have a rigid rodlike main chain decorated by short *and* long flexible side chains. The side chains, which are usually alkane chains, provide a "solvent" matrix in which the main chains are embedded. These molecules lie flat at the air−water interface adopting a 2D nematic-like, liquid crystalline state, which avoids crystallization and therefore defects, such as grain boundaries.[4]

The "hairy rod" polymers used in this study were modified polyglutamates containing short and long alkyl chain esters (Figure 1a,b). These molecules have been studied before with several different techniques (for a recent review see ref 5). Film balance studies[6] showed

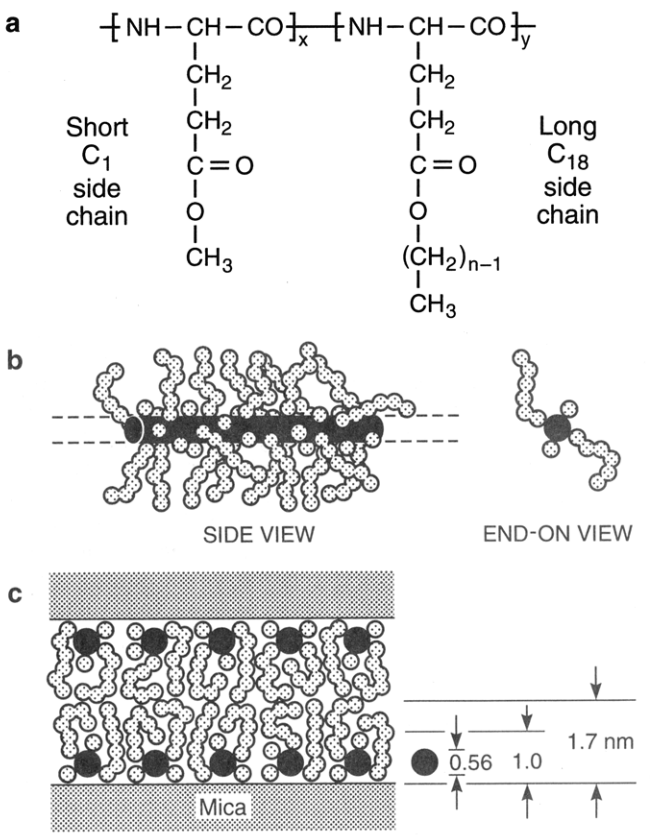

Figure 1. (a) Molecular formula of the used polyglutamates. The mole fraction of the long alkyl side chains is defined as y, and the mole fraction of the short side chain as x, with $x + y = 1$. The long alkyl side chain contains $n = 18$ C atoms and the short only one C atom. (b) Schematic representations of the molecular geometry in an isotropic bulk film. (c) Molecular conformation of the polyglutamates after transfer to a solid support (end-on view).

that these molecules form stable monolayers at the air−water interface, and that they can be transferred completely and repeatedly onto a solid support, allowing for the build up of well-ordered multilayered films up

† University of California.
‡ Max-Planck-Institute für Polymerforschung.
[⊗] Abstract published in *Advance ACS Abstracts,* March 15, 1995.

0024-9297/95/2228-3401$09.00/0

Table 1. Properties of the Polyglutamates (PG) Used

abbreviated name	mole fraction of long (C_{18}) side chain (y)	area per monomer (nm^2)	area per long side chain (nm^2)
PG_{30}	0.30	0.19	0.64
PG_{48}	0.48	0.22	0.45
PG_{66}	0.66	0.28	0.42

to 1 μm thick. These polyglutamate films show excellent optical properties, allowing for low loss (low defect) wave guiding, patterning, and information storage. Their internal structure was deduced by mainly X-ray and neutron scattering investigations, leading to the molecular conformation model discussed later (see Figures 1 and 7). Multilayers also showed an improved temperature stability as compared to conventional LB systems.[7,8]

Several recent papers addressed the structure and mobility of the side chains, which determine most of the polyglutamate properties. These measurements were performed at room temperature and the resulting model[4] describes the polyglutamates as molecular reinforced liquids or nanocomposites; this is based on experimental evidence that the side chains are in a fluid-like state whereas the main chain is rigid and thereby provides mechanical stability. Brillouin scattering experiments[9] have yielded the tensor elements of the elastic modulus and confirmed the molecular composite structure. Diffusion of small dye molecules within the side chain region of multilayers was fast on a small length scale.[10] Quartz crystal resonator experiments concluded that the side chains are partly in a glassy state.[11]

In this paper we investigated the adhesion (interfacial) energy, the micromechanical behavior, and the friction behavior of polyglutamate-coated surfaces. We measured and compared the forces between these surfaces, subjected to both normal and lateral movement. We were particularly interested in energy-dissipating processes that occur when the surfaces are moved and how these are influenced by the side chains. The relation between adhesion energy hysteresis and friction, which has been recently found for monolayer surfactant films,[12] was tested for the very different alkyl chain configuration encountered here, where the alkyl chains are covalently attached to a 1D polymer main chain rather than to headgroups attached to a surface. By varying the mole fraction (relative amounts) of the long and short side chains, it was possible to investigate the effect of chain density on the interfacial properties without changing the "headgroup", which in our case is the polymer main chain. If the side chains are in a fluid-like state, polyglutamate-coated surfaces should show very low friction that could possibly be used as an ultrathin, "dry" lubricant layer. All experiments were carried out with the surface forces apparatus (SFA),[13] which is ideally suited to measure the dynamic forces between, and deformations of, two interacting surfaces moving normally or laterally.

Materials and Methods

Materials. The material under investigation is poly(γ-methyl L-glutamate)$_x$-*co*-(γ-*n*-octadecyl L-glutamate)$_y$ whose alkyl side chains with carbon numbers $n = 1$ and $n = 18$ have mole fractions x and $y = (1 - x) = 0.30$, 0.48, and 0.66, as shown in Figure 1 and Table 1. The synthesis of these polyglutamates, to be referred to as PG_y, has been described elsewhere.[14-16] In the experimental temperature range 15–71 °C the polyglutamate main chain forms an α-helix, which

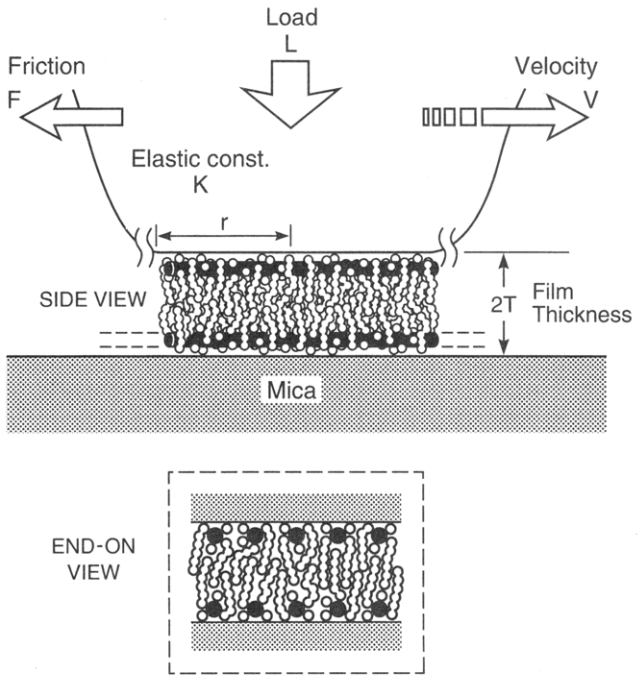

Figure 2. Schematic of the contact region in the adhesion energy hysteresis (variation of contact radius r *vs* load L) and friction experiments (friction force F at constant velocity V and load L). The lower inset shows the polyglutamates in an end-on view parallel to the sliding direction.

is very rigid and stable in this conformation until 150 °C.[17] The side chain of $n = 18$ C atoms, with 17 methylene $-CH_2-$ groups, is known to be long enough to cause interdigitation and crystallization in bulk samples[18,19] and LB films.[7]

Langmuir–Blodgett Deposition. Polyglutamate monolayers were prepared using a commercial film balance (Joyce-Loebl), whose temperature was held constant at 25 °C. The polymers were spread from a 0.5 mg/mL chloforom solution onto a subphase of pure water (Millipore), and the solvent was left to evaporate for 20 min. The monolayers were then compressed to a surface pressure of $\pi = 17$ mN/m and held constant at this pressure to check for stability. Suitable mica supports, previously immersed in the subphase before spreading the polyglutamates, were now withdrawn at a speed of 6 mm/min. When the supports passed through the air–water interface, a single polyglutamate monolayer was transferred with a transfer ratio of 1.00 ± 0.05. The transfer of molecules onto the solid support itself causes a two-dimensional alignment at the air–water interface, which induces the main chains to become deposited parallel to the dipping direction.[20]

Adhesion Force Measurements. The surface forces apparatus (SFA) used for the (time-dependent) adhesion force measurements was a standard SFA Mark II.[13,21] Generally, two cylindrical mica surfaces, each of a radius $R \approx 1$ cm, are positioned in a crossed cylinder configuration. The two surfaces are brought toward each other using several mechanical stages of increasing sensitivity. An optical technique using multiple beam interference fringes (FECO) is used to monitor the contact region of the surfaces. From the shape and the wavelength position of the FECO fringes, one can measure the radius R of the surfaces and the distance D between them. When the surfaces are in adhesive contact, they flatten as shown in Figure 2, and when they are pressed together by an externally applied load L, they deform elastically further, increasing their contact area. The flattened contact radius r (5%) and the polymer film thickness T (2 Å) were also measured with the FECO fringes to the accuracy indicated.

Adhesion energies γ were obtained from the measured pull-off forces L_S and also by measuring the contact radius *vs* load (r–L) dependence. From the pull-off force L_S, which is the force needed to separate two surfaces from contact, one can calculate the adhesion (or surface) energy γ using[22]

$$\gamma_S = L_S/3\pi R \quad (1)$$

where $\gamma_S = \gamma$ at equilibrium. The contact radius *vs* load curves were analyzed according to the equation of Johnson, Kendall, and Roberts (JKR)[23] which is applicable to the contacts of elastically deformable, adhesive surfaces:

$$r^3 = \frac{R}{K}[L + 6\pi R\gamma + (12\pi R\gamma L + (6\pi R\gamma)^2)^{1/2}] \quad (2)$$

Note that for nonadhering surfaces ($\gamma = 0$) the JKR equation becomes equal to the Hertz equation.[23] By measuring the contact radius with *increasing* load, eq 2 gives the "loading" adhesion energy γ_L, while with *decreasing* load it gives the "unloading" adhesion energy γ_{UL}. If the system is in true thermodynamic equilibrium at all stages of the loading/unloading cycle, the adhesion energies of the loading and unloading branches are the same ($\gamma_{UL} = \gamma_L$) and are also equal to γ. Otherwise, the loading/unloading cycle is hysteretic, energy is dissipated, the adhesion energies are different ($\gamma_{UL} > \gamma_L$), and we define the adhesion energy hysteresis as

$$\Delta\gamma = \gamma_{UL} - \gamma_L \quad (3)$$

In hysteretic systems, the force L_S and the corresponding energy γ_S to separate the surfaces is also larger than the expected equilibrium values given by eq 1, and γ_S is between γ_{UL} and γ_L. The contact radii as a function of load were obtained from video recordings of the FECO fringes and plotted as r^3 *vs* L.

The constant K describes the mechanical behavior of the elastically deforming supporting material, which in these experiments is a composite consisting of the silvered mica sheets and supporting glue layers. The value of K thus depends on the glue and mica thicknesses in a particular experiment and is typically of order 10^{13} mN/m^2.[24] K is roughly constant during one experiment done at the same temperature but can have small variations within a loading/unloading cycle due to the glue not being perfectly elastic.[25,26] It was important to establish that the hysteresis in the r^3 *vs* L curves measured on loading and unloading were due to a hysteresis in γ rather than K and also to establish how any variations in K could affect the inferred values of $\Delta\gamma$. For each cycle, the two unknown parameters γ and K of eq 2 were determined in two different ways: (i) γ and K were calculated, with their errors, by a least-squares fitting procedure (using KaleidaGraph, Synenergy Software), first for the loading branch and again for the unloading branch; (ii) a single (average) value of K was assumed for the whole cycle, and γ_L and γ_{UL} were fitted for the loading and unloading branches. The results for a typical experiment are depicted in Figure 3, showing that variations in K during a typical cycle were small (*i.e.*, $K_L \approx K_{UL} \approx K_{AV}$) and have only a small effect on the computed value of $\Delta\gamma$, which remains the same, within the quoted errors, when calculated by methods i or ii.

Friction Measurements. For the friction experiments we used a modified SFA with a sliding attachment.[27] This friction device consists of a motorized micrometer-driven translation stage and a double-cantilever spring supporting one of the surfaces. The deflection of this spring is measured by a strain gauge and is proportional to the resisting friction force. The strain gauge signal was recorded on a chart recorder according to ref 27.

Experimental Procedure. After the LB deposition of the polyglutamate monolayers onto mica, the surfaces were installed in the SFA. Care was taken to ensure (i) a crossed cylinder geometry and (ii) parallel mutual alignments of the polyglutamate main chains, *i.e.*, along the previous dipping direction (mounting error approximately 5 °C). The SFA chamber was then purged with dry nitrogen gas for 10 h and P_2O_5 was placed inside the chamber to ensure the desired atmospheric condition of 0% relative humidity (RH). The whole experimental room was kept at a fixed temperature T (±0.5 °C) in the range 15–35 °C, whereas for the higher temperatures (44–71 °C) the SFA was heated by two resistive heating rods that were inserted into the chamber.

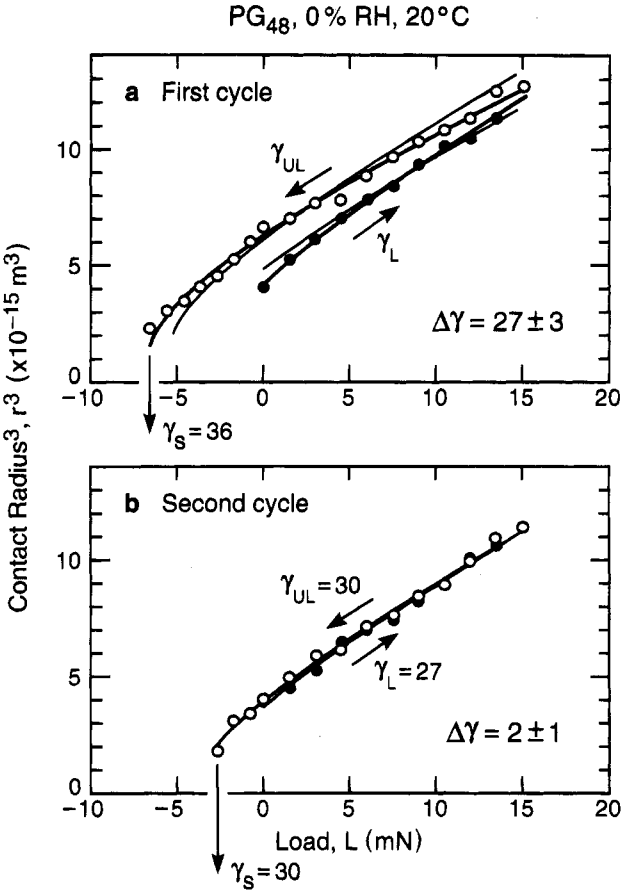

Figure 3. Contact radius versus load (r^3 *vs* L) curve for the polyglutamate PG_{48} at $T = 20$ °C and 0% RH. (a) First loading/unloading cycle. The fit according to eq 2 yields for the loading branch (thick line) $\gamma_L = 28 \pm 2$ mJ/m^2 and $K_L = 3.5 \times 10^{13}$ mN/m^2, and for the unloading branch (thick line) $\gamma_{UL} = 58 \pm 2$ mJ/m^2 and $K_{UL} = 4.2 \times 10^{13}$ mN/m^2, so that $\Delta\gamma = 30 \pm 4$ mJ/m^2. Using the average value of K obtained for the loading and unloading cycles, $K_{AV} = 3.8 \times 10^{13}$ mN/m^2, and fitting only γ (thin lines), we obtained $\gamma_L = 30 \pm 2$ mJ/m^2 and $\gamma_{UL} = 53 \pm 3$ mJ/m^2, so that $\Delta\gamma = 23 \pm 5$ mJ/m^2. The "pull-off" force, which is the force needed to separate the surfaces from contact, gave $\gamma_S = 36$ mJ/m^2. (b) Immediate second cycle after (a). The loading branch gives $\gamma_L = 27 \pm 2$ mJ/m^2 and $K_L = 3.7 \times 10^{13}$ mN/m^2, and the unloading branch $\gamma_{UL} = 30 \pm 1$ mJ/m^2 and $K_L = 3.9 \times 10^{13}$ mNm^2, so that $\Delta\gamma = 3$ mJ/m^2. Using again the average value of K, we obtained $\gamma_L = 27 \pm 1$ mJ/m^2 and $\gamma_{UL} = 28 \pm 1$ mJ/m^2, so that $\Delta\gamma = 1$ mJ/m^2. Here the two types of fits are practically indistinguishable, so that only one is shown. The "pull-off" force is $\gamma_S = 30$ mJ/m^2. These results, and others from different experiments and at different temperatures, are given in Figure 4.

Results

Molecular Conformation. At the air–water interface polyglutamates show a well-defined conformation due to their structural and chemical anisotropy: the polar α-helix lies flat on the water surface while the alkyl side chains try to avoid the water and so orient toward the air. All monolayers were compressed to the same surface pressure of $\pi = 17$ mN/m, but since the amount of the longer alkyl side chain affects the compressibility, the average area per alkyl chain was slightly different for different y values, falling in the range 0.19–0.28 nm^2/chain, as given in Table 1. The monolayers were transferred to the solid mica support with a transfer ratio of 1.00 ± 0.05. Previous X-ray and neutron-scattering experiments of polyglutamate mul-

tilayers have shown that the resulting conformation of a polyglutamate monolayer within a bilayer is as illustrated in Figure 1c, where the rigid α-helix main chain is 0.56 nm thick and is embedded in a 1.0 nm thick region of the short side chains and parts of the long side chains. The rest of the long alkyl side chains forms a less dense layer of thickness 0.7 nm, for PG_{30}.[7,28] Plasmon-surface-polariton measurements obtained a total thickness T of 1.7 nm for PG_{30} and 1.9 nm for PG_{66}.[6] The total thickness T of 1.7 ± 0.2 nm for PG_{30} was here independently confirmed by measuring the wavelength shift of the FECO fringes relative to the value for bare mica.

Adhesion Energy Hysteresis. When the surfaces approach in air, they "jump" spontaneously into adhesive contact as soon as the (attractive) force gradient exceeds the spring constant of the force-measuring spring.[13] Because of the adhesion, the initially curved surfaces deform to a flat contact area (see Figure 2) whose radius r is given by eq 2. Figure 3 shows typical contact radius *vs* load (r^3 *vs* L) curves for loading/unloading cycles of PG_{48} at 20 °C and 0% RH. For the first cycle (Figure 3a) the fit to eq 2 yields for the loading branch $\gamma_L = 28 \pm 2$ mJ/m^2 and $K_L = 3.5 \times 10^{13}$ mN/m^2, and for the unloading branch $\gamma_{UL} = 58 \pm 2$ mJ/m^2 and $K_{UL} = 4.2 \times 10^{13}$ mN/m^2; thus method i gives $\Delta\gamma = 30 \pm 4$ mJ/m^2. Using the average value of $K_{AV} = 3.8 \times 10^{13}$ mN/m^2 and fitting only γ, we obtained $\gamma_L = 30 \pm 2$ mJ/m^2 and $\gamma_{UL} = 53 \pm 3$ mJ/m^2, so that method ii gives $\Delta\gamma = 23 \pm 5$ mJ/m^2. Comparing these two values for $\Delta\gamma$, we see that they agree within the calculated errors (these values with their errors, together with other values for $\Delta\gamma$ obtained in other experiments and at different temperatures are shown in Figure 4b). The adhesion energy, which was also determined from the "pull-off" force L_S to separate the surfaces was $\gamma_S = 36$ mJ/m^2 (Figure 3a), which lies between and γ_L and γ_{UL}.

If, after separation, the surfaces are immediately brought back into contact and a second loading/unloading cycle is measured, the adhesion energy hysteresis was always found to be much smaller, as shown in Figure 3b, where $\Delta\gamma$ had fallen to 2 ± 1 mJ/m^2. Also, γ_S is now 30 mJ/m^2. Thus, all three values, γ_L, γ_{UL}, and γ_S, are now close to the expected thermodynamically reversible value for hydrocarbon surfaces, $\gamma = 23$–31 mJ/m^2, composed of CH_2 and CH_3 groups.[29–31] On further immediate contacts after separation, the behavior stays qualitatively the same and the hysteresis remains small.

Temperature Dependence. Figure 4 shows the temperature dependence of the adhesion energy hysteresis $\Delta\gamma$ for PG_{48} at 0% RH. The results in Figure 4a refer only to first contacts after transfer from the air–water interface and show a sharp maximum in $\Delta\gamma$ at $T \approx 60$ °C. The adhesion around 60 °C was so great that when the surfaces were brought together, the contact spread out rapidly, forming a very large contact area. Due to experimental limitations of accurately measuring very large γ values, we could not completely quantify the r^3 *vs* L behavior during the loading/unloading cycle at $T \approx 60$ °C, but qualitatively it exhibited by far the largest adhesion energy hysteresis.

A minimum in the adhesion energy hysteresis was found at 25 °C and $\Delta\gamma$ increased again toward smaller temperatures. We expect the existence of a second maximum at around 15 °C but could not locate it. As described above, immediate second and subsequent cycles all showed much reduced $\Delta\gamma$ and, especially in the range of $T = 15$–35 °C (Figure 4b), the adhesion energy hysteresis during repeat cycles was fairly constant and small (less than 5 mJ/m^2).

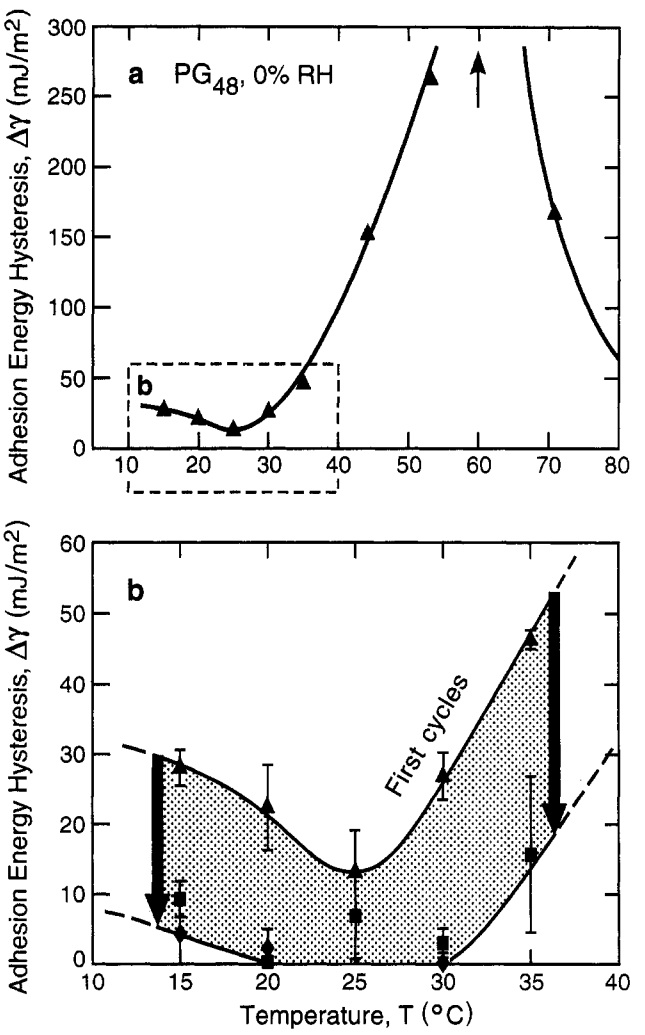

Figure 4. (a) Cumulative results from a number of experiments of the adhesion energy hysteresis on first contact for the polyglutamate $y = 0.48$ at 0% RH at various temperatures T. A maximum at about 60 °C, a minimum at 25 °C, and another increase toward smaller temperatures can be seen. (b) In the range 15–35 °C the differences between first (▲), immediate second (■), and immediate third (◆) loading/unloading cycles are shown.

Effect of Waiting Time. Figure 5 shows the effect of waiting time between contacts on $\Delta\gamma$. In these experiments, instead of bringing the surfaces back into contact immediately after a separation (as in Figure 4b), they were kept apart for various waiting times from minutes to hours before the adhesion cycle was repeated. It was found that many hours were needed before the surfaces returned to their original state of high adhesion energy hysteresis. Thus, at $T = 15$ °C, the initial hysteresis was $\Delta\gamma = 30$ mJ/m^2, falling to 10 ± 2 mJ/m^2 for zero waiting time, but rising to 17 ± 3 mJ/m^2 after the surfaces were kept apart for 12.5 h. Similarly, at $T = 30$ °C, after 13 h waiting time $\Delta\gamma$ was 22 ± 2 mJ/m^2, which was again higher than that after zero waiting time ($\Delta\gamma \approx 0$) and almost the same as the original hysteresis measured of $\Delta\gamma = 25$ mJ/m^2.

Rate and Load Effects. The rate of the advancing and receding contact area was varied by changing the time intervals between load increments. The rate can be expressed as a (radial) velocity and was constant in each experiment. In one series of experiments this rate

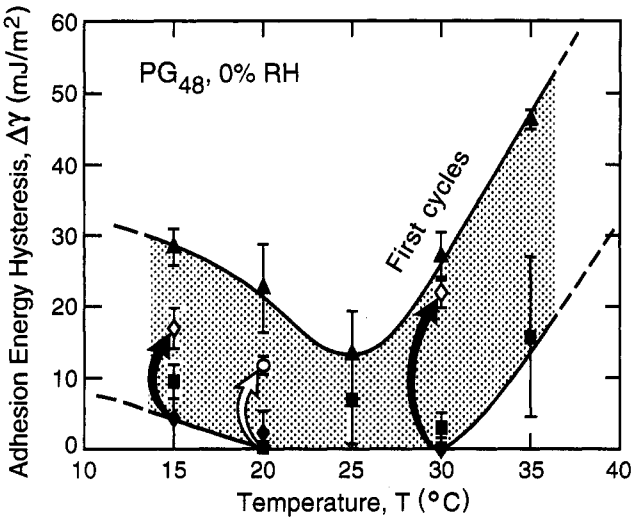

Figure 5. Additional to the data points of Figure 4b, the effects of increasing maximum load (○) and waiting time between contacts (◇) are shown.

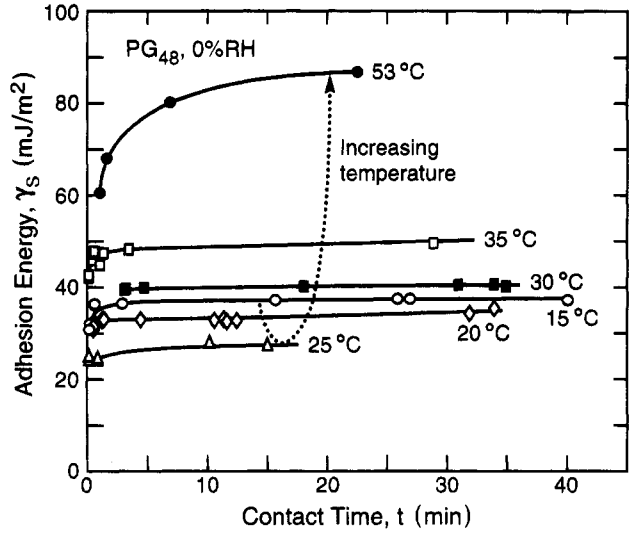

Figure 6. Dependence of the adhesion energy γ_S on the contact time t at various temperatures, without applying any load.

was decreased by a factor of 5, but no effect was observed on the loading and unloading adhesion energies (data not shown).

In Figure 5 we also show the effect of the maximum load in a loading/unloading cycle on the adhesion energy hysteresis. Whereas in all other experiments the maximum load was 15 mN on the first and all subsequent adhesion cycles, in one experiment at $T = 20$ °C we increased the maximum load to 21 mN during the second (immediate) cycle. Instead of the "expected" hysteresis $\Delta\gamma \approx 0 \pm 3$ mJ/m^2, we obtained $\Delta\gamma = 12 \pm 1$ mJ/m^2 (white arrow at $T = 20$ °C).

Pull-Off Forces. The adhesion energy γ_S, as determined from the force necessary to separate the surfaces without going through a loading/unloading cycle, can also be studied as a function of contact time. The results are depicted in Figure 6 for PG_{48} at different temperatures. The adhesion energy γ_S is smallest at $T = 25$ °C and increases at smaller temperatures ($T = 20$, 15 °C) as well as at higher temperatures ($T = 30$, 35, 53 °C). The time that the surfaces are allowed to remain in contact (with or without applying a load) was also found to have a characteristic influence on γ_S. For most of

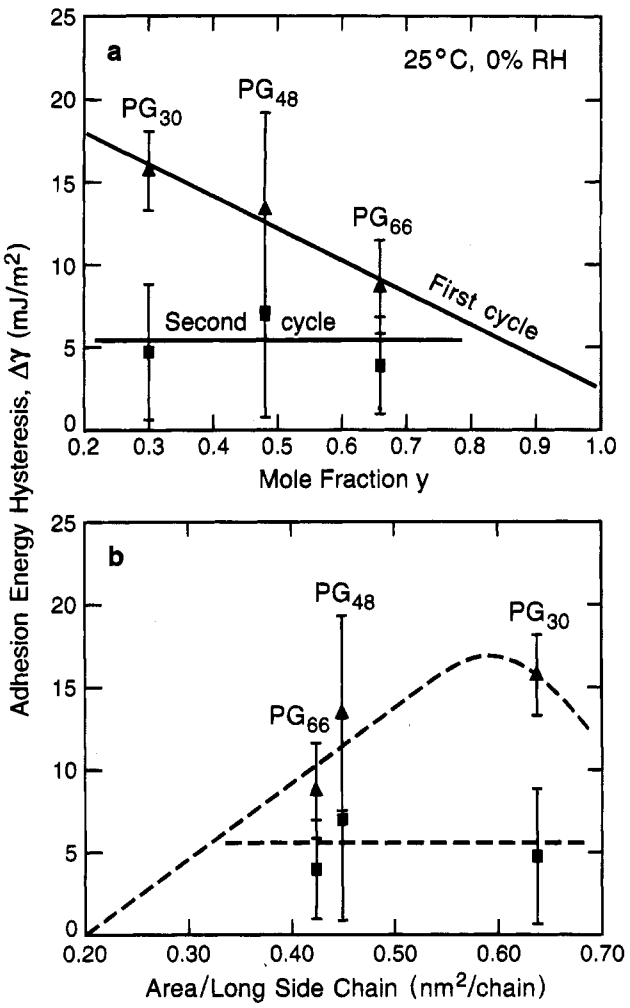

Figure 7. (a) Adhesion energy hysteresis for three different polyglutamates on first (▲) and immediate second (■) loading/unloading cycles. The solid lines are linear fits. (b) Same data plotted again the average area per long side chain. The dashed lines are a guide to the eye.

the temperatures the adhesion energy increases rapidly for small contact times and approaches a plateau for longer contact times. The exception is at $T = 25$ °C, where no initial fast increase was observed.

Effect of Side Chain Density. In a second series of experiments we used polyglutamates with different long side chain densities. Figure 7a shows the adhesion energy hysteresis $\Delta\gamma$ of the polyglutamates PG_{30}, PG_{48}, and PG_{66} with a long side chain mole fraction of $y = 0.30$, 0.48, and 0.66 taken at $T = 25$ °C and 0% RH. Note that the data for PG_{48} is the same as in Figure 4. We see that with increasing mole fraction of the long alkyl chain $\Delta\gamma$ decreases for the first cycles but is roughly the same for the immediate second cycles. By expressing the same data in terms of the area per long side chain (see Table 1 and Figure 7b) the trends are unchanged. These effects are analyzed in the Discussion.

Friction Measurements. In a third set of experiments we investigated the tribological properties of polyglutamate monolayers using the SFA friction attachment. The monolayer-coated surfaces were mounted so that the sliding direction was parallel to the dipping direction, i.e., the direction of the main chain (see Figure 2). If it were perpendicular, the molecules would presumably roll and the molecular (surface) geometry would be different. Figure 8 shows a set of typical

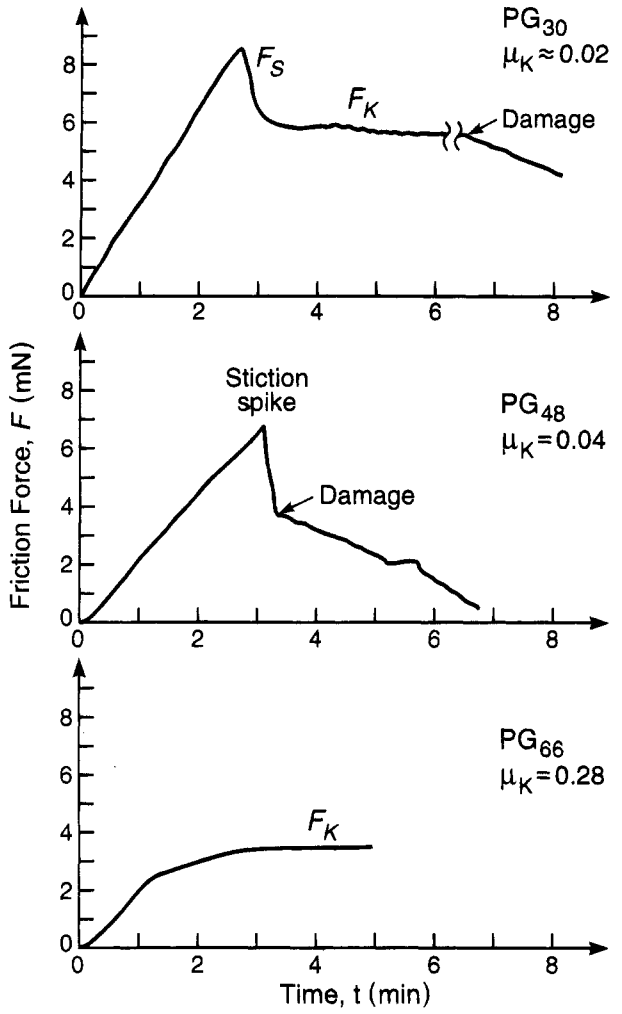

Figure 8. Friction traces (friction force F *vs* time t) for the three different polyglutamates. The polyglutamates that are strongly interacting (PG_{30}, PG_{48}) show high static friction F_S, often causing damage, and high kinetic friction F_K, whereas the polyglutamate with the smallest adhesion energy hysteresis (PG_{66}) exhibits only sliding in a kinetic friction mode.

friction traces, giving the friction force F as a function of time t. Sliding starts at time $t = 0$. The ambient conditions were $T = 25$ °C, 0% RH, and the loads and velocities were comparable to those used in the adhesion hysteresis experiments. If the translation stage moves and the two surfaces stick together, the supporting spring deflects and the friction force F increases linearly with time. The slope of this curve is then mainly determined by the elastic modulus of the spring and therefore cannot be used to obtain the modulus of the film material. When the stress reaches a yield point, which is typical for friction behavior, the surfaces begin to move. If the initial motion is a rapid "slip", it is called "stiction" and was found for the polyglutamates PG_{30} and PG_{48} (see Figure 8). After the first slip, the surfaces usually continue to slide smoothly and steadily (kinetic friction with no stick-slip), which gives rise to a horizontal line on the friction trace. This occurred between surfaces coated with PG_{30}, whereas in the case of PG_{48} the first slip after stiction usually caused damage which forced the surfaces to separate from molecular contact and the friction force to fall with time. Monolayers of PG_{66}, while showing smooth kinetic sliding, exhibited no stiction spike on starting.

We also measured the dependence of the kinetic friction force F_K on the applied load, which showed a linear behavior. The slope is often used to define a friction coefficient μ, which was 0.02 for PG_{30}; $\mu = 0.04$ for PG_{48} and $\mu = 0.28$ for PG_{66}.

Discussion

Molecular Mechanism of the Adhesion Energy Hysteresis. The contact radius *vs* load curve shown in Figure 3 for PG_{48} shows a strong hysteresis on loading and unloading. This behavior is qualitatively the same for all the polyglutamates studied. The adhesion energy for the loading branch is $\gamma_L = 28$ mJ/m^2, which is as expected for surfaces exposing alkyl chains[29-31] (surfaces composed mainly of CH_3 groups have $\gamma = 23$ mJ/m^2, and surfaces with mainly CH_2 groups have $\gamma = 31$ mJ/m^2). We conclude that the energetics during the loading is well described by the equilibrium surface energy ($\gamma_L = \gamma$) arising from the van der Waals interaction between the hydrocarbon groups at the interface.

In contrast, the measured adhesion energy for the unloading branch, $\gamma_{UL} = 58$ mJ/m^2, was much higher. Since the van der Waals energy depends on the molecular contact area, the higher value for γ_{UL} during unloading can be attributed to an increase—approximately doubling—of the molecular contacts. Considering the conformation of the polyglutamate monolayers, this increase in molecular contacts can be explained by an interpretation or interdigitation of the long alkyl side chains. This behavior is thus very similar to what has recently been observed with surfactant and lipid monolayers,[12,22] where adhesion energy hysteresis was high if the monolayers were (i) not in the totally fluid nor totally solid state, and (ii) able to interdigitate on contact. It was shown earlier that only a small amount (*i.e.*, a few angstroms) of interpenetration was sufficient to cause a significant adhesion energy hysteresis.[12] Theoretical work has also indicated that large energy dissipation can arise from only a small zone of interdigitation between two moving polymer brush layers.[32]

Molecular Chain Ordering, Relaxations, and Memory Effects. If the surfaces are brought back into contact immediately (within minutes) after separation, the adhesion energy hysteresis is much smaller (*cf.* Figure 4b), due mainly to a decrease in γ_{UL}, that is, in the unloading branch—the loading surface energy γ_L remaining unchanged and equal to γ. This shows that the interfaces behave more like normal hydrocarbon surfaces at equilibrium after being separated from contact and implies that the interdigitation process, that led earlier to an increase in the van der Waals contacts, is now prevented or that the time to interdigitate and de-interdigitate has been changed. Tentatively, we attribute this effect to an ordering of the long alkyl side chains induced during the first loading/unloading cycle and separation of the contact. On immediate third and subsequent cycles, the behavior did not change and the adhesion energy hysteresis remained close to zero. It is well-known that well-oriented and close-packed alkyl chains do not interpenetrate and show no or little adhesion energy hysteresis.[12,22] Such a close packing can be obtained even when the chains are less dense than in the crystalline phase (approximately 0.20 nm^2/chain for alkanoic acids[1]) by stretching and uniformly tilting relative to the surface normal. In the case of alkanethiols, tilt angles of 30° on gold[1] and 55° on GaAs[33] have been observed, reflecting the ability of alkyl chains to accommodate to different surface densities. Figure 9 summarizes the model of the molecular con-

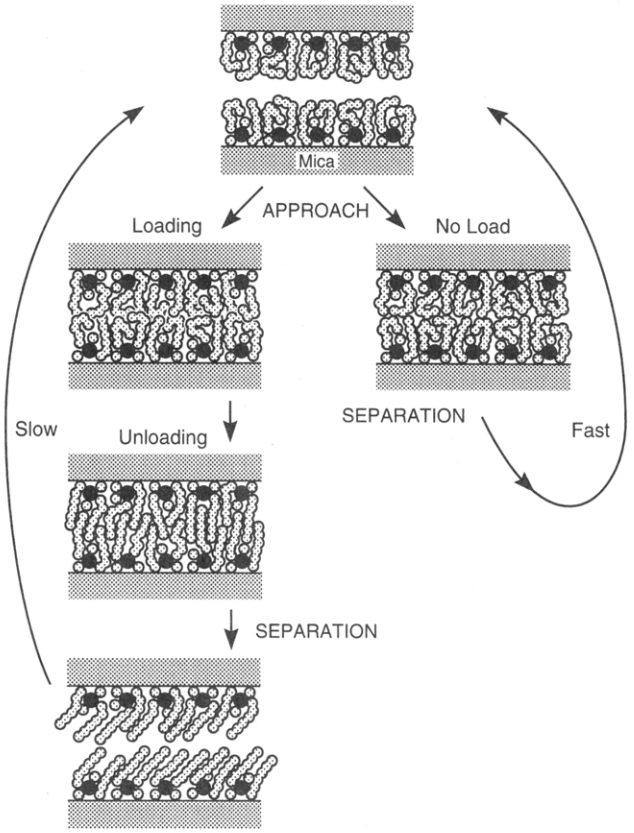

Figure 9. Proposed schematic model of the interaction between polyglutamate monolayers. When going through a loading/unloading cycle (left) the long side chains interdigitate and remain in a stretched and tilted conformation after separation. Without a load application, and particularly for short contact times, the side chains remain in their original disordered state during contact (right).

formations before and after the first loading/unloading cycle (see also the Conclusion).

Because the ordering of the long alkyl side chains is artificially induced, one expects it to relax back to the more random original state after a certain time. As mentioned in the results section (*cf.* Figure 5), this was indeed observed. After waiting for ~12 h after a separation, $\Delta\gamma$ at 15 °C was significantly higher and at 30 °C it had nearly recovered to its original value. Since these relaxation times are very long, the long alkyl side chains are presumably in some frozen or amorphous state; this is not unreasonable considering that the melting points of octadecane and octadecanol, which have similar alkyl chains, are 28 and 59 °C, respectively. The relaxation process back to the original state may also be a cooperative one, involving a whole assembly of molecules, rather than a single one. Especially for a tilted, close-packed phase, this is very reasonable. If we had waited even longer, the polyglutamate monolayers would presumably have relaxed completely. The faster relaxation rate observed at the higher temperature is consistent with an activated molecular relaxation process. Currently, we cannot say if rearrangements of the polymer main chain also influence the relaxation behavior for which further studies are needed. To this end, we are planning a series of infrared spectroscopy experiments to investigate the dynamic conformational changes at the molecular level.

Also related to the time effects discussed above is the effect of the loading and unloading rates. Previously, it had been shown that the adhesion energy hysteresis generally decreases as the loading/unloading rate decreases.[22] We varied the rate by a factor of 5, but no effect was seen on $\Delta\gamma$. Apparently, compared to the characteristic relaxation time which is of the order of hours (see above), these rates, which were on the order of minutes, were too fast to have had an effect on $\Delta\gamma$. Had the unloading rate been reduced to several hours, we could have expected the adhesion energy hysteresis to also decrease. In the limit of infinitely long cycle times, which means approaching true equilibrium conditions, the hysteresis $\Delta\gamma$ should completely vanish.

Effects of Load and Temperature on Adhesion Energy Hysteresis. By going through a loading/unloading cycle with a higher maximum load, one forces the two surfaces closer together, enhances the interdigitation, and increases the maximum contact area. This resulted in an increased $\Delta\gamma$, as was observed experimentally at 20 °C (see Figure 5). In the case of surfactant monolayers, this behavior was observed before[22] and attributed to a nonuniform stress distribution. According to the JKR theory, the compressive stress is highest inside the contact region, leading to enhanced interdiffusion at this point. This effect can also be viewed in the context of the recently introduced "friction" or "energy loss phase diagrams":[12] In a representation of energy loss *vs* temperature as shown in Figure 4a, an increase in maximum load corresponds to *shifting of the whole curve* relative to the temperature (and $\Delta\gamma$) axes to higher temperatures, or in other words to *performing the experiment* at a lower temperature. We see that the adhesion energy hysteresis increases as we move toward lower temperatures. One may further speculate that the motion that leads to interdigitation and the reverse motion of de-interdigitation are influenced differently by load. It is reasonable to suppose that interdigitation or chain "mixing" is enhanced, but the de-interdigitation or "demixing" is slowed down by an increased load, which is readily seen to act like a *decreased* temperature.

The temperature dependence of the adhesion energy hysteresis, as shown in Figure 4, can also be viewed as an energy loss spectrum or phase diagram of the polyglutamate monolayers. The larger the hysteresis, the more energy is put into the system and used up to peel the polyglutamate layers apart. As mentioned above, the adhesion energy hysteresis is caused mainly by the interdigitation of the long alkyl side chains. However, more than one molecular process may lead to interdigitation, and the different processes may have different characteristic relaxation or activation temperatures, leading to a complex temperature dependence of the energy dissipating processes.[34] Experimentally, this is expected to show up as a series of maxima in the energy dissipation–temperature spectrum and in the adhesion energy hysteresis and friction curves, each located at the characteristic temperature for each process (which is also a function of the load, velocity, or frequency of the measurement). In the case of bulk polymer systems this behavior is well-known; see for example Ferry's monograph.[34]

Comparison with Previous Work. Our data can be compared with previous studies on polyglutamates, where other techniques that also measure energy loss spectra were used. These include calorimetry,[18] mechanical[18] and dielectric spectroscopy,[35] and NMR.[36] These measurements were all performed on bulk samples and with polyglutamates that contained the same long side chain (n = 18) but a mole fraction of y = 1.00

(homopolymer). When comparing the data, one should also keep in mind the differences in sample preparation: In a bulk sample of mole fraction $y = 1.00$ the side chains are oriented toward both sides of the main chain, so that only about 50% "point" in one direction. In our monolayer preparation *all* the long side chains are pointing away from the solid support, so that our polyglutamate monolayer with $y = 0.48$ should be comparable to a bulk sample of higher long side chain density, *i.e.*, to a polyglutamate with $y \approx 2 \times 0.48 = 0.96$, or $y \approx 1.00$.

Watanabe *et al.*[18] found a transition at 60 °C in mechanical relaxation and calorimetry experiments and showed that this transition involves the melting of the long alkyl side chains. Romero Colomer *et al.*[35] confirmed the melting transition of the interdigitated side chains at $T \approx 60$ °C and found, with dielectric spectroscopy, a β-relaxation at ~20 °C and a γ-relaxation at even lower temperatures. Mohanty *et al.*[36] measured the relaxation times of NMR signals and also found a melting transition at $T \approx 60$ °C and a γ-relaxation at $T < 0$ °C, whose exact location depended on the frequency used.

For $y = 0.48$ at 0% RH we located a maximum in the adhesion energy hysteresis at $T \approx 60$ °C, a minimum at $T = 25$ °C and a further increase at smaller temperatures. Although we could not locate a second maximum at small temperatures due to experimental limitations, we expect its existence at around $T = 15-20$ °C. The shape of our energy loss–temperature spectrum in the range of 15–50 °C for polyglutamate monolayer films resembles very much the energy loss spectrum for bulk polyglutamate samples, as shown in Figure 8 of ref 35. The nature of the involved molecular processes in bulk samples was recently revealed by a combination of X-ray, dielectric spectroscopy, and NMR experiments:[19] The γ-relaxation corresponds to a restricted twisting motion of the carboxyl dipoles and the β-relaxation is a glass transition of the ester groups in the side chains (see Figure 1). The outer parts of the long side chains contain amorphous and crystalline parts that melt at a temperature close to 60 °C; the exact temperature depends on the side chain density. It appears that the same molecular motions that cause the melting of the crystalline side chains in bulk samples at $T \approx 60$ °C lead to interdigitation and maximum energy dissipation at the same temperatures in monolayers. At 25 °C these processes are not (yet) active, no or little interdigitation occurs, and we find a minimum in the adhesion energy hysteresis. The molecular motions, that are active at smaller temperatures and cause the glass transition in bulk samples, lead to interdigitation and an increase in $\Delta\gamma$ at $T = 15-20$ °C in our monolayer experiments. Since these processes involve only a partial mobility of the long side chains (segments), the resulting interdigitation is less pronounced and the measured $\Delta\gamma$ is smaller than that at $T \approx 60$ °C.

The adhesion energy γ_S without going through the loading/unloading cycle (Figure 5) at $T = 25$ °C is typical for hydrocarbon surfaces, but it is the smallest for all temperatures. At all other temperatures the adhesion is bigger and follows the same trends as the adhesion energy hysteresis. We conclude that at all temperatures except 25 °C molecular interdigitation processes are active, which increase the molecular contacts and thereby the adhesion energy. Especially the process that leads to the initial fast increase in adhesion is absent at 25 °C, so that only a small and slow increase is observed.

Effect of Short and Long Side Chain Densities. Since the feasibility of chain interdigitation depends on the area that each chain occupies, it was instructive to vary the density y of the long side chains. This was achieved by using a set of molecules with varying copolymer composition, ranging from $y = 0.30$ to 0.66 (Table 1). As mentioned in the results section (and Figure 7a) at 25 °C the adhesion hysteresis for the first contact *decreases* linearly with the *increasing* mole fraction of the long side chain. If we extrapolate this trend, we see that the adhesion energy hysteresis would become zero at a mole fraction of $y = 1.1 \pm 0.1$. This is very reasonable, since a homogeneous close-packed array of identical side chains would prevent mutual interpenetration and/or reduce the number of segment rearrangements that could occur on contact. We can quantify this analysis by transforming the long side chain density from a mole fraction into an area per long side chain. In Figure 7b we see that the adhesion energy hysteresis decreases with decreasing area per long side chain. If we extrapolate the data, we find that the hysteresis would be zero at an area of about 0.20 nm^2/chain. This is as expected since this is the value for close packed alkyl chains attached to polar headgroups[1] and at closest packing no interdigitation is possible.

To achieve optimum interdigitation and adhesion energy hysteresis, the chains have to fulfill a geometrical requirement *and* a particular mobility to interdigitate and deinterdigitate. Assuming a homogeneous distribution of the long alkyl side chains on both surfaces, the geometric requirement for maximum interdigitation occurs at double the closest packing area, or 0.40 nm^2/long side chain. But to also ensure the necessary mobility of the chains, they need a larger area per chain than the purely geometric requirement. On the other hand, if the density of the chains gets too small (area too high), interdigitation becomes less favorable and the molecular interaction and hysteresis between the side chains will decrease. Therefore, we expect the adhesion energy hysteresis to have a maximum at a certain area per long side chain. These conclusions are supported by the experimental results (see Figure 7b): PG_{66} fulfills the geometrical requirement but does not have enough mobility. The area per long chain, and therefore the mobility, is increased at PG_{48}, and we find a higher adhesion energy hysteresis. PG_{30} shows only a slightly increased value, because the area per long side chain is now already much higher than 0.40 nm^2/chain. We expect a maximum in the adhesion energy hysteresis at a mole fraction between $y = 0.48$ and 0.30 (*cf.* dashed line for first cycles in Figure 7b).

Relation between Adhesion Energy Hysteresis and Friction. In the following discussion of the measured friction behavior, we show that the friction and adhesion energy hysteresis are related in this system. The alignment of the polymer main chain along the sliding direction ensured that the tribological behavior was dominated by the side chain interactions: when one of the surfaces moves, the long side chains could slide past each other without moving the main chain. But the film always ruptures at its weakest point. So, when the interaction between the side chains is too strong, *i.e.*, when it becomes stronger than the PG–mica interaction, the film ruptures irreversibly (Figure 8) and the surfaces will separate. Experimen-

tally, we observed this behavior for PG_{48} and PG_{30}, which were the molecules that also exhibited the highest friction forces and adhesion energy hysteresis. The polyglutamate with the lowest adhesion energy hysteresis, PG_{66}, also showed a qualitatively different friction behavior. Because the long side chain density is higher, the monolayers interdigitate less and therefore slide more easily past each other. Consequently, we observed no stiction and stable kinetic friction, without damage.

It is possible to quantitatively predict either the friction force F or the adhesion energy hysteresis $\Delta\gamma$ of a certain system, if we know one or the other of the above quantities. In order to do this, we have to assume that in both cases, the same molecular processes lead to the energy dissipation.[37] Here, we identified interdigitation of the long alkyl side chain as the responsible molecular mechanism/process which is possible in normal (adhesion) as well as in lateral (friction) motion. In either movement direction, molecules are brought into contact and then separated.[37] In such cases, we can equate the dissipated energy ΔE as[12]

$$\Delta E(\text{adhesion energy hysteresis}) = \Delta E(\text{friction})$$

or

$$\Delta\gamma A = Fl \tag{4}$$

where A is the contact area, F is the friction force, l is the molecular interaction length, and $\Delta\gamma$ is the adhesion energy hysteresis measured under similar conditions.[37] Actually, we expect $F < \Delta\gamma A/l$ because during frictional sliding the van der Waals "bonds" are not completely broken, as occurs on separation (to infinity) in adhesion experiments. For the interaction length we used l = 20 Å, which is approximately the maximum extension of a long alkyl side chain ($n = 18$). Applying eq 4 to the PG_{48} monolayers at 25 °C, using $\Delta\gamma$ = 13 mJ/m^2 (see Figure 7a), $A = \pi(25\ \mu\text{m})^2$ (with $r = 25\ \mu$m taken from the r^3 *vs* L curve), and l = 20 Å, the predicted friction force is F = 13 mN. For PG_{30} at 25 °C, using $\Delta\gamma$ = 16 mJ/m^2 (see Figure 7a), $A = \pi(25\ \mu\text{m})$,^{2} and l = 20 Å, the predicted friction force is F = 15 mN. These predictions are less than, but in order of magnitude agreement with, the measured friction forces of 4 and 6 mN, respectively (see Figure 8). With the above assumptions, the uncertainty in the measured values (*i.e.*, averaged molecular area, estimated interaction length), the obtained agreement is remarkably good, especially considering the simplicity of eq 4.

The friction force or coefficient should likewise be interpretable in terms of a "friction" or "energy loss phase diagram".[37] Since we measured the adhesion energy hysteresis for PG_{48} at different temperatures, the shape of the energy loss phase diagram for this molecule is known. The friction coefficient corresponds to the slope of the energy loss curve with increasing load or by shifting the energy loss curve toward higher temperatures. Since we measured a minimum in the adhesion energy hysteresis and therefore in the energy loss curve, at that temperature where the friction coefficient was measured (T = 25 °C), the energy loss increases only a little and the friction coefficient is small. We can also make predictions about the shape of the energy loss curve for the other polyglutamates used. Since the friction coefficient for PG_{30} is also small, we expect a similar shape of the energy loss curve and a minimum in the adhesion energy hysteresis at T = 25 °C. Because PG_{66} has a higher friction coefficient, the minimum in energy dissipation at T = 25 °C should be either less shallow or its position should be shifted toward higher temperatures.

Conclusions

Our proposed model for the molecular conformational changes during PG monolayer interactions is schematically depicted in Figure 9. When spread at the air–water interface, polyglutamates adopt an asymmetrical configuration, with the α-helix in contact with the water and the long alkyl side chains trying to avoid the water by pointing toward the air. Because of the "dilution" with the short side chains the long side chains are in a disordered and flexible state.

When two deposited PG monolayer surfaces come into contact without applying a load, the polyglutamates initially interact with their outer methyl groups and exposed methylene moieties. After this fast contact is established (see Figure 6), the chains rearrange slowly to adopt the most energetically favorable conformation, as seen in the slow increase of the adhesion energy in Figure 6. After separation the chains relax back into their original conformation so that the behavior is repeatable on further contacts (Figure 9, right).

The situation is different when the surfaces are in prolonged contact and a loading/unloading cycle is applied (Figure 9, left). During the loading the side chains are pressed further together, but the initial (loading) interaction is still characterized by the "normal" or equilibrium adhesion energy for hydrocarbon surfaces. On unloading, the situation changes qualitatively: by pulling the now highly interdigitated surfaces apart, the chains stretch out until they finally separate. Because of the uniform stretching, the long alkyl chains adopt a new and more ordered conformation, for example, by tilting uniformly. This ordered, induced state relaxes only very slowly back to its original, disordered conformation, but on immediate recontacts the interdigitation is low and so is the adhesion energy hysteresis.

When subjected to normal and lateral motions, the surfaces dissipate energy which results in adhesion energy hysteresis and (kinetic) friction, respectively. Assuming that the same molecular processes cause the energy dissipation during both movements, we have introduced an equation that quantitatively relates the adhesion energy hysteresis $\Delta\gamma$ to the friction force F.

The temperature dependence of the adhesion energy hysteresis of PG monolayers was found to be very similar to bulk samples. At least for this monolayer system, the behavior of quasi two-dimensional monolayers only a few angstroms thick is therefore seen to be not very different compared to three-dimensional bulk samples. The reason being that the properties in both cases are dominated by the interactions of the long side chains and that these are similar, despite the dimensionality.

The semi-empirical WLF equation allows for the description of various relaxation and energy dissipating phenomena at different temperatures, pressures (loads), and velocities (frequencies, inverse time), using the time–temperature superposition principle.[34] Applying this concept to monolayer interactions, we expect the energy dissipation curves to shift to different temperatures when different loads or velocities (time) are used. The validity of the WLF equation for describing the relaxation processes has already been demonstrated in bulk samples[19] of "hair rod type" polymers and has been

theoretically proposed for two-dimensional systems.[38] Our (preliminary) results indicate the validity of this for the highly complex PG monolayer system, and we plan to vary the velocity and other relevant parameters systematically in future experiments in order to check the superposition principle and the general applicability of energy loss phase diagrams to monolayers in greater detail.

Acknowledgment. This research was supported by the Department of Energy (DOE) under grant DE-FG03-87ER45331. The development of the instrumentation was funded by the National Science Foundation (NSF) under the Materials Research Laboratory (MRL) grant DMR 91-23048.

References and Notes

(1) Ulman, A. *An introduction to ultrathin organic films. From Langmuir-Blodgett to self-assembly*; Academic Press Inc.: San Diego, 1991.
(2) Swalen, J. D.; Allara, D. L.; Andrade, J. D.; Chandross, E. A.; Garoff, S.; Israelachvili, J.; McGarthy, T. J.; Murray, R.; Pease, R. F.; Rabolt, J. F.; Wynne, K. J.; Yu, H. *Langmuir* **1987**, *3*, 932.
(3) Orthmann, E.; Wegner, G. *Angew. Chem.* **1986**, *98*, 189.
(4) Wegner, G. *Thin Solid Films* **1992**, *216*, 105.
(5) Wegner, G. *Mol. Cryst. Liq. Cryst.* **1993**, *235*, 1.
(6) Hickel, W.; Duda, G.; Jurich, M.; Kroehl, T.; Rochford, K.; Stegeman, G. I.; Swalen, J. D.; Wegner, G.; Knoll, W. *Langmuir* **1990**, *6*, 1403.
(7) Vierheller, T. R.; Foster, M. D.; Schmidt, A.; Mathauer, K.; Knoll, W.; Wegner, G. *Macromolecules* **1994**, *27*, 6893.
(8) Schmidt, A.; Mathauer, K.; Reiter, G.; Foster, M. D.; Stamm, M.; Wegner, G.; Knoll, W. *Langmuir* **1994**, *10*, 3820.
(9) Nizzoli, F.; Hillebrands, B.; Lee, S.; Stegeman, G. I.; Duda, G.; Wegner, G.; Knoll, G. *Phys. Rev. B* **1989**, *40*, 3323.
(10) Schaub, M. Diploma Thesis, University Mainz, 1990.
(11) Johannsmann, D.; Mathauer, K.; Wegner, G.; Knoll, W. *Phys. Rev. Lett., B: Condens. Matter* **1992**, *46*, 7808.
(12) Yoshizawa, H.; Chen, Y.-L.; Israelachvili, J. *J. Phys. Chem.* **1993**, *97*, 4128.
(13) Israelachvili, J. N. *Surf. Sci. Rep.* **1992**, *14*, 109.
(14) Duda, G. Ph.D. Thesis, University Mainz, 1988.
(15) Duda, G.; Schouten, A. J.; Arndt, T.; Lieser, G.; Schmidt, G. F.; Bubeck, C.; Wegner, G. *Thin Solid Films* **1988**, *159*, 221.
(16) Duda, G.; Wegner, G. *Makromol. Chem. Rapid Commun.* **1988**, *9*, 495.
(17) Arndt, T.; Wegner, G. In *Optical Techniques To Characterize Polymer Systems*; Bässler, H., Ed.; Elsevier: Amsterdam, 1989; p 41.
(18) Watanabe, J.; Ono, H.; Uematsu, I.; Abe, A. *Macromolecules* **1985**, *18*, 2141.
(19) Schmidt, A.; Lehmann, S.; Georgelin, M.; Katana, G.; Mathauer, K.; Kremer, F.; Schmidt-Rohr, K.; Boeffel, C.; Knoll, W.; Wegner, G *Macromolecules*, submitted.
(20) Schwiegk, S.; Vahlenkamp, T.; Xu, Y.; Wegner, G. *Macromolecules* **1992**, *25*, 2513.
(21) Israelachvili, J. N. *Intermolecular and surface forces*; Academic Press: London, 1991.
(22) Chen, Y.-L.; Helm, C. A.; Israelachvili, J. N. *J. Phys. Chem.* **1991**, *95*, 10736.
(23) Johnson, K. L.; Kendall, K.; Roberts, A. D. *Proc. R. Soc. London, Ser. A* **1971**, *324*, 301.
(24) Horn, R. G.; Israelachvili, J. N.; Pribac, F. *J. Colloid Interface Sci.* **1987**, *115*, 480.
(25) Greenwood, J. A.; Johnson, K. L. *Phil. Mag. A* **1981**, *43*, 697.
(26) Maugis, D. *J. Mater. Sci.* **1985**, *20*, 3041.
(27) Homola, A.; Israelachvili, J.; Gee, M. L.; McGuiggan, P. M. *J. Tribol.* **1989**, *111*, 1.
(28) Schmidt, A. Ph.D. Thesis, University Mainz, 1992.
(29) Zisman, W. A. *J. Colloid Sci.* **1952**, *7*, 428.
(30) Zisman, W. A. *Ind. Eng. Chem.* **1963**, *55*, 19.
(31) Fowkes, F. M. *Ind. Eng. Chem.* **1964**, *56*, 40.
(32) Joanny, J.-F. *Langmuir* **1992**, *8*, 989.
(33) Wade Shen, C.; Shi, J.-X.; Martensson, J.; Parikh, A. N.; Allara, D. L. *J. Am. Chem. Soc.* **1992**, *114*, 1514.
(34) Ferry, J. D. *Viscoelastic Properties of Polymers*; John Wiley & Sons: New York, 1980.
(35) Romero Colomer, F.; Gómez Ribelles, J. L.; Lloveras Maciá, J.; Muñoz Guerra, S. *Polymer* **1991**, *32*, 1642.
(36) Mohanty, B.; Watanabe, J.; Ando, I.; Sato, K. *Macromolecules* **1990**, *23*, 4908.
(37) Israelachvili, J. N. In *CRC Handbook of Micro/Nanotribology*; CRC Press: Boca Raton, FL, 1995; Chapter 8.
(38) Wittmann, H.-P.; Kremer, K.; Binder, K. *Makromol. Chem., Theory Simul.* **1992**, *1*, 275.

MA946061X